ISSN 1674-1056
http://cpb.iphy.ac.cn
http://iopscience.iop.org/cpb
中国物理 B
Chinese Physics
中国物理 Chinese Physics B

Analysis of the fractal intrinsic quality in the ionization of Rydberg helium and lithium atoms

Yanhui Zhang(张延惠), Xiulan Xu(徐秀兰), Lisha Kang(康丽莎), Xiangji Cai(蔡祥吉), Xu Tang(唐旭)
Citation: Chin. Phys. B . 2018, 27(5): 053401. **doi:** 10.1088/1674-1056/27/5/053401

Journal homepage: http://cpb.iphy.ac.cn; http://iopscience.iop.org/cpb

What follows is a list of articles you may be interested in

Production of projectile and target *K*-vacancy in near-symmetric collisions of 60-100 MeV Cu^{9+} ions with thin Zn target

Yipan Guo(郭义盼), Zhihu Yang(杨治虎), Shubin Du(杜树斌), Hongwei Chang(常宏伟), Qingliang Xia(夏清良), Qiumei Xu(徐秋梅)
Chin. Phys. B . 2016, 25(3): 033401. **doi:** 10.1088/1674-1056/25/3/033401

Resonance enhanced electron impact excitation for P-like Cu XV

Li Shuang, Yan Jun, Li Chuan-Ying, Huang Min, Chen Chong-Yang
Chin. Phys. B . 2015, 24(11): 113401. **doi:** 10.1088/1674-1056/24/11/113401

Charge transfer of He^{2+} with H in a strong magnetic field

Liu Chun-Lei, Zou Shi-Yang, He Bin, Wang Jian-Guo
Chin. Phys. B . 2015, 24(9): 093402. **doi:** 10.1088/1674-1056/24/9/093402

Scaling law of single ion-atom impact ionization cross sections of noble gases from He to Xe at strong perturbative energies

Ren Ping-Yuan, Zou Xian-Rong, Shao Jian-Xiong, Wang Shi-Yao, Zhou Man, Zhou Wang, Yang Ai-Xiang, Yan Peng-Xun, Chen Xi-Meng
Chin. Phys. B . 2015, 24(6): 063402. **doi:** 10.1088/1674-1056/24/6/063402

Multiple ionization of Ne induced by 10 keV/u-500 keV/u C^{q+} (q=1-3) ions

Liu Wen-Biao, Niu Shu-Tong, Yang Ai-Xiang, Han Cheng-Zhi, Hu Wei, Chen Lin, Shao Jian-Xiong, Chen Xi-Meng
Chin. Phys. B . 2015, 24(6): 063403. **doi:** 10.1088/1674-1056/24/6/063403

Analysis of the fractal intrinsic quality in the ionization of Rydberg helium and lithium atoms*

Yanhui Zhang(张延惠)[1,†], Xiulan Xu(徐秀兰)[1], Lisha Kang(康丽莎)[1], Xiangji Cai(蔡祥吉)[2], and Xu Tang(唐旭)[1]

[1] College of Physics and Electronics, Shandong Normal University, Jinan 250014, China
[2] School of Physics, Shandong University, Jinan 250100, China

(Received 5 August 2017; revised manuscript received 12 January 2018; published online 26 April 2018)

We study the fractal rhythm in the ionization of Rydberg helium and lithium atoms in an electric field by using the semiclassical method. The fractal structures present a nested relationship layer by layer in the initial launch angles of the ionized electrons versus the escape time, which is defined as the rhythm attractor, and exhibit similar rhythm endings. The gradually enhanced chaotic regions of the escape time plots tend to broaden as the scaled energy increases. In addition, the fractal rhythm changes synchronously with the oscillations of the kinetic energy spectrum. We note that the intrinsic quality of the fractal rhythm is closely related to the kinetic energy distribution, that is, the inherent dynamic properties of the Hamiltonian equations have an impact on the fractal regularities. In addition, different ionizing closed trajectories exhibit iterate properties and the inherent beauty of symmetry. Our results and analysis can not only reveal new laws in the ionization of Rydberg atoms, but also promote the establishment of the dynamic mechanism of fractals.

Keywords: ionization dynamics, Rydberg atoms, fractal rhythm, kinetic energy spectrum

PACS: 34.50.Fa, 05.45.Pq, 03.65.Sq **DOI:** 10.1088/1674-1056/27/5/053401

1. Introduction

In recent years, nonlinear science, especially chaos theory, has revealed the universality of the fractal structure in physics. Chaotic phenomena exist in many research fields, such as the escape dynamics of particles in mesoscopic devices, the ionization of high excited atoms, and so on.[1–7] The interaction between lasers and matter is an important means to explore new laws of microstructures.[8–13] The emergence and development of atomic physics in extreme strong field conditions can not only reveal new physical phenomena and effects, promote the progress of the ultra-fast laser, but also enable people to truly understand molecules, atoms, and their internal properties.[14–18]

With the advancement of laser technology and semiclassical theory, considerable attention has been paid to photoionization microscopy and the ionization dynamics of atoms in external fields.[2,6,7,19–25] The chaotic ionization of hydrogen in electric and magnetic fields is described by the Poincaré map.[26–29] Recently, with the development of chaos and fractal theory in physics, consideration has been given to fractal dynamics in many fields, for example, the fractal dynamics in quantum and semiclassical transport.[12,30–35] The escape dynamics of trapped ultracold atoms and Bose–Einstein condensates always exhibit fractal features.[36–38] What is more, diverse attractors exist in nonlinear systems, such as the limit cycle attractor, torus attractor, Lorenz attractor, strange attractor, and so on, which all reflect the diversity of the nature and the flexuosity in the process of evolution. The ionization of Rydberg atoms is one of the most interesting fields in chaos and fractal physics. It is notable that, for the ionization of multi-electron Rydberg atoms in external fields, the intrinsic quality of fractal remains unrealized. Hence, it is a challenge to find the correspondence between the fractal mechanism and the chaotic escape laws of electrons in ionization systems.

In the present paper, we study the intrinsic quality of the fractal in the ionization of Rydberg helium and lithium atoms in an electric field and define the rhythm attractor to analyze the fractal structures within the framework of the semiclassical closed orbit theory.[8,9] Moreover, we study the influence of the potential energy distribution on the chaotic extent of the ionized electrons and calculate the kinetic energy spectra, which show excellent synchronism to the fractal structures. The symmetrical and iterative properties of the typical closed trajectories are discussed to reveal the dynamic mechanism of fractals within the ionization process of Rydberg atoms.

The paper is organized as follows. In Section 2, we briefly review the ionization process and the potential energy distribution. In Section 3, we discuss the relationship between the fractal rhythm of the escape time plots and the kinetic energy spectra, and the iterative and symmetrical features of the classical closed trajectories for both helium and lithium atoms.

*Project supported by the Natural Science Foundation of Shandong Province, China (Grant No. ZR2014AM030). Xiangji Cai is also partially supported by the Program for Outstanding PhD Candidate of Shandong University, China.

†Corresponding author. E-mail: yhzhang@sdnu.edu.cn

© 2018 Chinese Physical Society and IOP Publishing Ltd

Section 4 presents the conclusions of the present paper.

2. Semiclassical closed-orbit theory

2.1. Ionization mechanism and the potential

Due to the fact that Rydberg atoms are very sensitive to external fields, we consider helium Rydberg atoms (with only one excited electron) and lithium atoms placed in an electric field directed along the z-axis, respectively. Within the framework of the closed-orbit theory, the outgoing wave packet which propagates away from the atomic core can be described as the evolution of ensemble electron trajectories.[8,9,13] In cylindrical coordinates (ρ, z), the ionization schematic view of the Rydberg system is depicted in Fig. 1. When a laser pulse strikes the atom, the excited electron moves outward from the nucleus in all directions, following the classical trajectories and being turned around by the external field, which are shown by the black solid lines in Fig. 1. Eventually the escaping electrons form a concentric wave packet interference pattern on the detector plane.

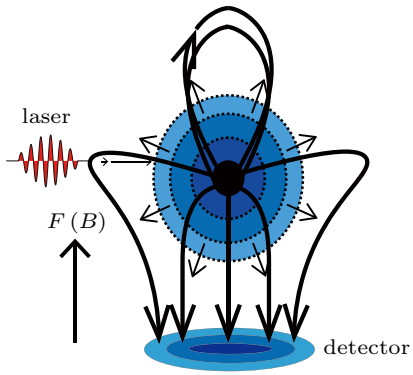


Fig. 1. Schematic of some classical trajectories in the process of the ionization of a Rydberg atom which is placed in an electric field F (or magnetic field B) that is oriented along the z axis and perpendicular to the detector plane. If the ionized electron absorbs a photon, the electron moves away from the nucleus with its initial outgoing angle, and the waves propagate outward in all directions. Some trajectories head directly downhill, other trajectories head uphill initially and then return to the nucleus. Thus, the outgoing wave can be described as an ensemble of classical trajectories.

The Hamiltonian of highly excited electrons in helium atoms with an electric field oriented along the z-axis can be written as

$$H\left(\rho, z, p_\rho, p_z\right) = \frac{1}{2}\left({p_\rho}^2 + {p_z}^2\right) + V(\rho, z) + Fz, \qquad (1)$$

where F is the electric field strength, and the z component of the angular momentum is taken to be zero. $V(r,z)$ is the Hüpper model potential written as[4,19]

$$\begin{aligned} V(\rho,z) &= V_{\text{Coulomb}}(\rho,z) + V_{\text{core}}(\rho,z) \\ &= -\frac{1}{(\rho^2+z^2)^{1/2}} - \frac{Z-1}{(\rho^2+z^2)^{1/2}} \\ &\quad \times \left(1+\frac{(\rho^2+z^2)^{1/2}}{a}\right) \exp\left[\frac{-(\rho^2+z^2)^{1/2}}{a}\right], \end{aligned} \qquad (2)$$

where $Z = 2$ is the nuclear charge, and $a = 1/3$ is the parameter of the model potential determined by the range of the ion core for the helium Rydberg atom.[19]

By the scaling law $\widetilde{r} = rF^{1/2}$, $\widetilde{P} = PF^{-1/4}$, $\widetilde{\varepsilon} = EF^{-1/2}$, and $\widetilde{t} = tF^{3/4}$, the transformed Hamiltonian can be written as

$$\begin{aligned} \widetilde{H} &= \frac{1}{2}(\widetilde{P}_\rho^2 + \widetilde{p}_z^2) - \frac{1}{\widetilde{P}_\rho^2 + \widetilde{p}_z^2} - \frac{Z-1}{(\widetilde{P}_\rho^2+\widetilde{p}_z^2)^{1/2}} \\ &\quad \times \left(1+\frac{(\widetilde{\rho}^2+\widetilde{z}^2)^{1/2}}{a}\right) \exp\left[\frac{-(\widetilde{\rho}^2+\widetilde{z}^2)^{1/2}}{a}\right] + \widetilde{z}. \end{aligned} \qquad (3)$$

The Coulomb singularity of the above Hamiltonian can be eliminated through adopting semiparabolic coordinates (u, v) and conjugate momenta (p_u, p_v) which are respectively given by

$$\begin{aligned} u &= (\widetilde{r}+\widetilde{z})^{1/2}, \quad v = (\widetilde{r}-\widetilde{z})^{1/2}, \\ p_u &= \widetilde{p}_\rho v + \widetilde{p}_z u, \quad p_v = \widetilde{p}_\rho u - \widetilde{p}_z z. \end{aligned} \qquad (4)$$

The new scaled time variable is $\mathrm{d}t = (u^2+z^2)\mathrm{d}\widetilde{t}$, and the regularized Hamiltonian can be given by introducing an effective form $h = 2\widetilde{r}(\widetilde{H} - \varepsilon)$

$$\begin{aligned} h(u,v,p_u,p_v) &= \frac{1}{2}({p_u}^2 + {p_v}^2) + V(u,v) - 2, \\ V_{uv} &= -\varepsilon(u^2+v^2) + \frac{1}{2}(u^4 - v^4) \\ &\quad - 2\left(1+\frac{u^2+v^2}{2a}\right)\exp\left(-\frac{u^2+v^2}{2a}\right) + 2. \end{aligned} \qquad (5)$$

Atomic units $\hbar = |e| = m_{\text{eff}} = 1$ are used here and in the following. Clearly, the model potential is controlled by the scaled energy ε. By using analogous scaling laws[27–29], for the lithium Rydberg atom in electric fields, the regularized Hamiltonian of the electron has a similar form.[19]

In order to show how the electrons escape in the ionization process, we depict the potential energy distribution of the Rydberg helium and lithium atoms at the same scaled energy $\varepsilon = -1.3$ in Figs. 2(a) and 2(b), respectively. The atoms are located at the center of the potential $u = v = 0$, the potential fields at the same coordinate range exhibit different structures. There are two obvious saddle points on the left and right sides of the counter plot of helium in Fig. 2(a), while the saddle points of lithium are not so obvious, which indicates that the potential well of lithium is relatively deeper and the core scattering effect is stronger than that of helium. Therefore, the ionized electrons escaping from the potentials will show different dynamical and chaotic features. The form of the Hamiltonian given in Eq. (5) is symmetric with respect to the coordinates u

and v, which denotes that the electronic dynamics for the Rydberg atoms in the external fields will present unique properties, as discussed in the following.

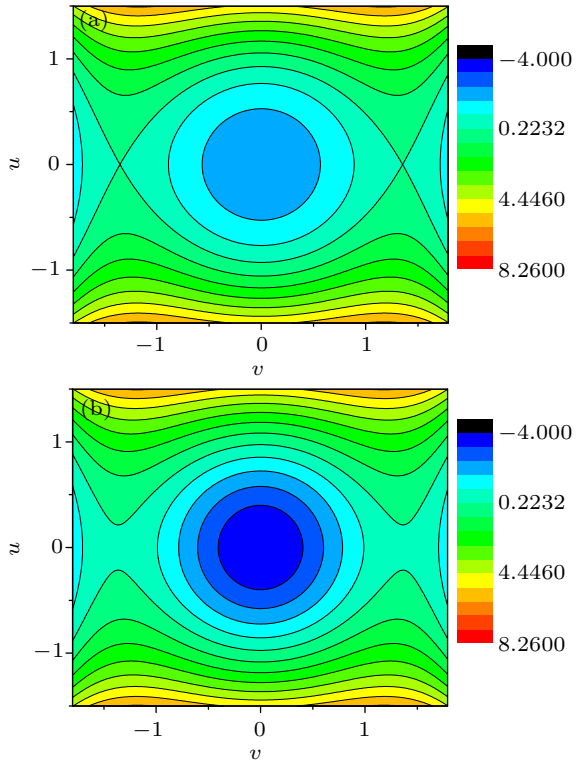


Fig. 2. Contour plots of the potential energy distribution of Rydberg (a) helium and (b) lithium atoms. The ionized electrons begin at the nucleus located at $u = v = 0$, and eventually pass over the saddle region, and escape from the well.

2.2. Fractal and chaotic attractors

Three successive magnifications of the escape time plots (icicle map) for the helium atom are shown in Figs. 3(a)–3(c). Figure 3(b) is the magnification of the angle interval between 1.4865 and 1.51737 of Fig. 3(a). Figure 3(c) is the magnification between 1.4946 and 1.50175 of Fig. 3(b). By analyzing the three different colored lines, the nested relationship layer by layer from Fig. 3(a) to Fig. 3(c) depicts the rhythm properties in the escape time plots. The fractal dimension $D_{\mathrm{f}} = \lim\limits_{R\to\infty} \frac{\lg N(R)}{\lg R}$ of the self-similarity structure can reflect the chaotic properties of the ionized electrons, which is calculated

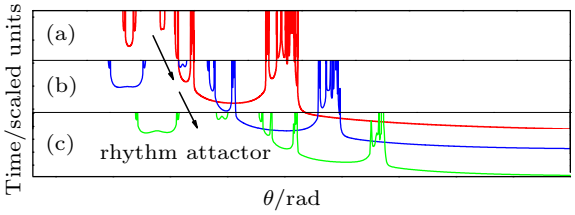


Fig. 3. Fractal self-similarity structures in the process of the ionization of a Rydberg helium atom placed in an electric field $F = 19$ V/cm. Three successive magnifications of the escape time plots: panel (b) is the magnification of the assigned angle interval of the fractal structures in panel (a), and panel (c) is the magnification of the assigned angle interval of the fractal structures in panel (b).

within the framework of the box-counting method.[20] We define the phenomena in the ionization systems as the rhythm attractor with the fractal dimension $D_{\mathrm{f}} = 0.467$ which expresses the irregularity of the rhythm structures. These curves exhibit the same rhythm at the endings of the plots, which are called "rhythm endings" denoting the universality in the ionization process.

3. Results and discussion

3.1. Fractal and chaotic structures of the escape time plots

In order to identify the rhythm properties in the ionization process, we compute the Hamiltonian motion of the Rydberg helium and lithium atoms based on the canonical equations, which are written as

$$\dot{q}_j = -\frac{\partial H}{\partial p_j}, \quad \dot{p}_j = -\frac{\partial H}{\partial q_j}. \tag{6}$$

With the initial conditions $u(t=0) = 0$, $v(t=0) = 0$, $p_u = 3.464\cos(\theta/2)$, and $p_v = 3.464\sin(\theta/2)$ of the lithium atom, we perform iterative calculations, obtain

$$\begin{aligned} \dot{u} &= p_u, \quad \dot{v} = p_v, \\ \dot{p_u} &= 2\varepsilon u - 2u^3 - 4\frac{u}{a}\exp\left(-\frac{u^2+v^2}{2a}\right), \\ \dot{p_v} &= 2\varepsilon v + 2v^3 - 4\frac{v}{a}\exp\left(-\frac{u^2+v^2}{2a}\right), \end{aligned} \tag{7}$$

and search the ionization trajectories in any outgoing angles. The iterative calculation has been widely used in researching the transport and ionization problems in the semiclassical field.

In Fig. 4, we compare the escape times and the initial launch angle ranges at different scaled energies $-1.7 \le \varepsilon \le -1.3$ for the lithium atom.

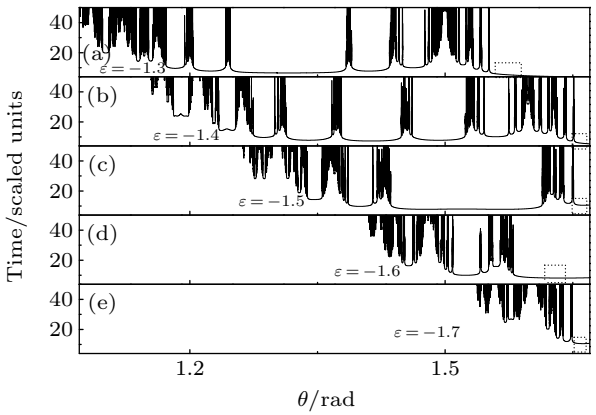


Fig. 4. Escape time plots for different energies ($-1.7 \le \varepsilon \le -1.3$) of lithium atoms in an electric field $F = 19$ V/cm. The ionization process shows chaotic characteristics and the dotted rectangles exhibit the same rhythm endings. The chaotic complexity regions become narrower with the decrease of the scaled energy.

We use the escape time curve, which is called the icicle map,[27–29] to provide more detailed insight into the connection between the fractal structure and the escape processes of

the ionized electrons. As shown in Figs. 4(a)–4(e), with the decrease of the scaled energy, the fractal icicle distribution shifts toward larger initial launch angles with the maximum escape time 50, and the chaotic complexity regions become narrower at the same time. This implies that the ionized probability decreases when the scaled energy decreases, and the electrons of larger ejection angles will be easier to reach the detector plane exhibiting more chaotic escape properties. These escape time plots contain the rhythm attractors and the dotted rectangles exhibit the same rhythm endings. Moreover, there are fractal self-similarity structures in the various scale ranges.

Considering the core scattering effect on the chaotic escape of electrons for the lithium atom, we further study the ionization of the helium Rydberg atom in a pure electric field at the scaled energy $\varepsilon = -1.3$. As shown in Figs. 5(a) and 5(b), the escape time plots display the same fractal self-similarity characteristics. Some electron trajectories head directly downhill to the detector plane within a short time, while other trajectories are turned around by the influence of the electric field. However, the chaotic regions in Fig. 5(b) show more sophisticated structures than those in Fig. 5(a), which suggests that the core scattering effect causes the enhancement of the ionization probability for the lithium atom under the same external conditions. The position of the fractal self-similarity region A in Fig. 5(a) is located in a finite interval $1.49693 \leq \theta \leq 1.50412$ and region B in $1.52405 \leq \theta \leq 1.53304$ as shown by the dashed line regions, respectively.

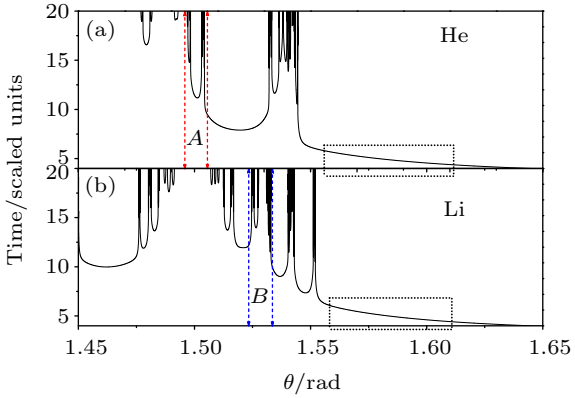


Fig. 5. For Rydberg atoms in an electric field $F = 19$ V/cm, the escape time that electrons take to strike the detector is plotted as a function of the initial launch angle at the same scaled energy $\varepsilon = -1.3$. (a) The escape time plot of the helium atom, chaotic region A is the typical fractal self-similarity region. (b) The escape time plot of the lithium atom, chaotic region B is the typical fractal self-similarity region. The dotted rectangles exhibit the same rhythm endings.

We next calculate the kinetic energy spectrum of families of ionizing trajectories. Figures 6(a) and 6(b) correspond to region A of Fig. 5(a). Figures 6(c) and 6(d) correspond to region B of Fig. 5(b). Clearly, the fractal rhythm in Figs. 6(a) and 6(c) and the kinetic energy oscillations in Figs. 6(b) and 6(d) exhibit excellent synchronous variations, respectively. The regions marked by the red lines from $a1$ to $e1$ in Fig. 6(a) correspond exactly to the chaotic positions of the escape time plot, the non-chaotic region between $a1$ and $b1$ corresponds to the non-chaotic kinetic energy oscillation. The regions marked by the blue lines from $a2$ to $g2$ in Fig. 6(c) show that the oscillations of the kinetic energy spectrum of Fig. 6(d) are changing synchronously with the fractal rhythm of different ionized electrons of Fig. 6(d). The intrinsic quality of the fractal rhythm is closely related to the energy distribution, that is, the inherent dynamical properties of the Hamiltonian affect the fractal regularities.

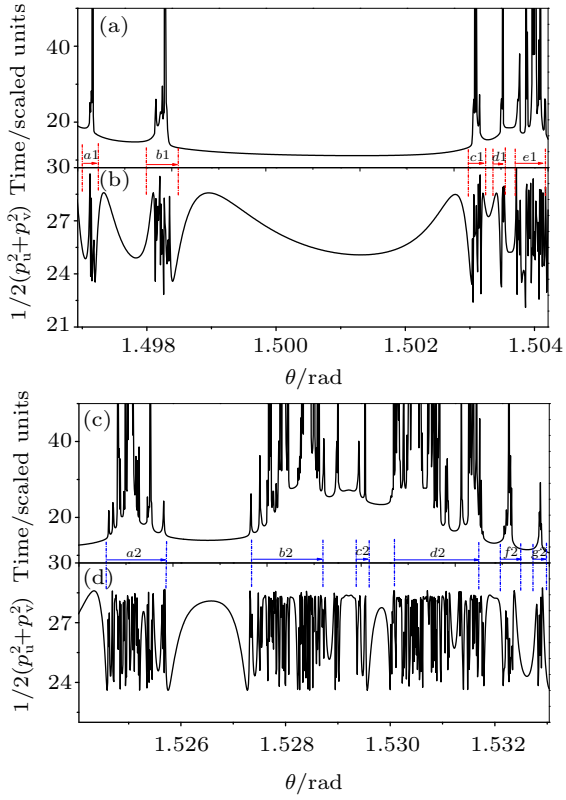


Fig. 6. (a) The fractal structures and (b) the kinetic energy spectra of the helium atoms; the kinetic energy oscillations exhibit excellent synchronous variations with the fractal rhythm as shown in the regions marked by red lines from $a1$ to $e1$. (c) The fractal structures and (d) the kinetic energy spectra for the lithium atoms; the kinetic energy oscillations exhibit excellent synchronous variations with the fractal rhythm as shown in the regions marked by red lines from $a2$ to $g2$.

Moreover, figures 6(c) and 6(d) of the lithium atom illustrate enhanced chaotic properties compared to those of the helium atom shown in Figs. 6(a) and 6(b), implying that the electronic dynamics is more complex, which is caused by the deeper ionization potential well than that of the helium atom. Since one point presents one classical trajectory in the escape time plots, and the plots show fractal regularity structures related to the kinetic energy spectrum, we shall see that classical trajectories in this system must contain certain properties, which will be discussed next.

3.2. Symmetry analysis of classical ionizing electron trajectories

To get a deeper insight into the fractal and the classical trajectories, we calculate the closed trajectories of the ionized electrons of the helium and lithium atoms.

In principle, all the initial outgoing angles should be examined, but we find that the Hamiltonian has a symmetry about z and the ionized electrons escape from the atom in all directions. Therefore, the trajectories can be obtained to research the fractal rhythm in the ionization process. We calculate the fractal dimensions of the escape time plots at different scaled energies for both the helium and the lithium atoms to study the escape behavior of the ionized electrons. For the helium atom, the fractal dimensions of the escape time plots are $D_{\rm f} = 0.52261, 0.51111, 0.49659, 0.47643, 0.43744$ at different scaled energies ($-1.3 \leq \varepsilon \leq -1.7$), respectively. The results indicate that the fractal dimensions decrease with the scaled energy, at the same time, the ionization of the helium atom shows enhanced chaotic characteristics. A set of ionizing closed trajectories of the helium and lithium atoms at the scaled energy $\varepsilon = -1.3$ are shown in Fig. 7. For the helium atom, from Fig. 7(a) to Fig. 7(c) we find that the three trajectories have similar iterative rules and present interesting rhythm properties. Moreover, the evolutional trends in Figs. 7(d)–7(f) tend to complexity step by step with the increasing number of crossings of the z-axis. The fractal dimensions of the escape time plots for the lithium atom in Figs. 4(a)–4(e) are $D_{\rm f} = 0.66299, 0.65249, 0.63716, 0.61537, 0.58623$, respectively. The fractal dimensions decrease with the decreasing scaled energy, moreover, the ionization of the lithium atom exhibits enhanced chaotic properties compared with that of the helium atom. In Fig. 7, the ionizing closed trajectories show perfect symmetry and iterative characteristics for the lithium atom, just like those of the helium atom. With the fractal dimensions calculated above, at the scaled energy $\varepsilon = -1.3$, $D_{\rm f}$ of the lithium atom is larger than that of the helium atom, which demonstrates that the trajectories of the lithium atom are more complex than those of helium. Because of the stronger core effects of the lithium atom, the dynamical motion of the ionized electrons is iterated numerically in the regularized coordinates, and iterate more and more times from Fig. 7(g) to Fig. 7(l). With a small variation of the initial launch angles, the trajectories show great disparities,[26,27] implying that the ionization of the Rydberg atom satisfies the basic rule of the chaotic system: sensitivity to the initial conditions.

Such rules of closed trajectories and fractal structures occur in many angles, which indicates the scale-free features in the ionization process. The symmetrical shapes of the closed trajectories and the rhythm reflect that the Hamiltonian equations influence the intrinsic dynamics of the ionization systems.

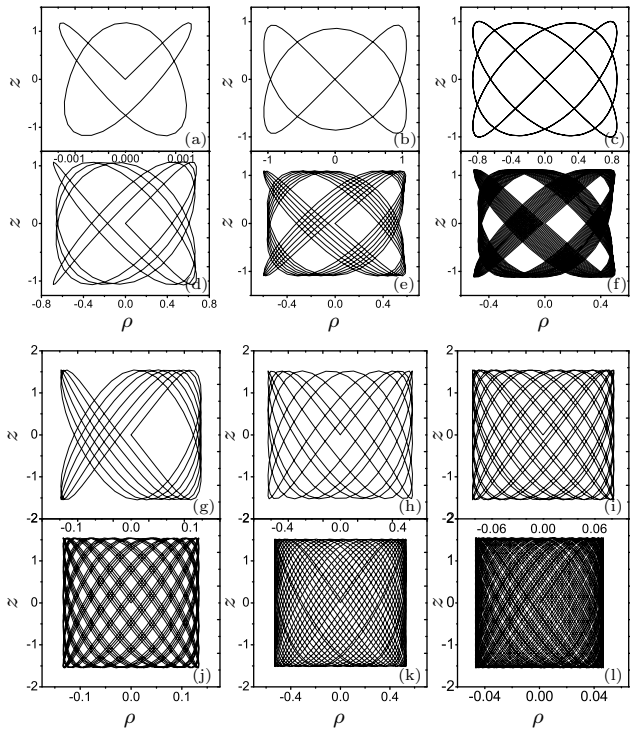


Fig. 7. Important typical types of closed trajectories of (a)–(f) helium and (g)–(l) lithium atoms in an electric field. Different trajectories are calculated for the two atoms, the panels (a)–(l) show the similar iterative rules and interesting rhythm properties.

4. Conclusion

In summary, we have used the semiclassical closed-orbit theory to calculate the ionization fractal rhythm of Rydberg helium and lithium atoms in an electric field. The fractal structures exhibit the nested relationship layer by layer which is defined as the rhythm attractor and present similar rhythm endings in the initial launch angles versus the escape time. Due to the energy distributions of the potentials being distinct, the scattering effects of the helium and lithium atoms show different dynamical impacts on the electrons. In addition, the ionization chaotic regions of the escape time plots tend to broaden as the scaled energy increases for the Rydberg atoms. Oscillations in the kinetic energy spectra of the helium and lithium atoms show excellent correspondence with the fractal structures, which illustrates that the intrinsic dynamic properties of the Hamiltonian equations are closely related to the fractal rhythm. The typical ionizing closed trajectories have been calculated and show iterate properties and perfect symmetry. We believe this work will provide more research methods for revealing new laws in the ionization of Rydberg atoms.

References

[1] Yang G C, Mao J M and Du M L 1999 *Phys. Rev. A* **59** 2053
[2] Zhao L B and Delos J B 2010 *Phys. Rev. A* **81** 053417

[3] Zhao L B and Delos J B 2010 *Phys. Rev. A* **81** 053418
[4] Hüpper B, Main J and Wunner G 1996 *Phys. Rev. A* **53** 744
[5] Lankhuijzen G M and Noordam L D 1996 *Phys. Rev. Lett.* **76** 1784
[6] Zhou H, Li H Y, Gao S, Zhang Y H, Jia Z M and Lin S L 2008 *Chin. Phys. B* **17** 4428
[7] Wang D H 2011 *Chin. Phys. B* **20** 013403
[8] Du M L 1989 *Phys. Rev. A* **40** 4983
[9] Du M L and Delos J B 1988 *Phys. Rev. A* **38** 1896
[10] Du M L and Delos J B 1987 *Phys. Rev. Lett.* **58** 1731
[11] Fabian L, Iva Březinová, Joachim B and Florian L 2013 *Phys. Rev. E* **88** 022916
[12] Zhao G P, Zhang Y H, Cai X J, Xu X L and Kang L S 2016 *Physica E* **84** 10
[13] Yang B C, Delos J B and Du M L 2014 *Phys. Rev. A* **89** 013417
[14] Blondel C, Delsart C and Dulieu F 1996 *Phys. Rev. Lett.* **77** 3755
[15] Nicole C, Offerhaus H L, Vrakking M J J, Lépine F and Bordas C 2002 *Phys. Rev. Lett.* **88** 133001
[16] Lépine F, Bordas C, Nicole C and Vrakking M J J 2004 *Phys. Rev. A* **70** 033417
[17] Nicole C, Sluimer I, Rosca-Pruna F, Warntjes M, Vrakking M, Bordas C, Texier F and Robicheaux F 2000 *Phys. Rev. Lett.* **85** 4024
[18] Ivanov I A, Nam C H and Kim K T 2016 *Phys. Rev. A* **93** 043404
[19] Hüpper B, Main Jörg and Wunner G 1995 *Phys. Rev. Lett.* **74** 2650
[20] Xu X L, Zhang Y H, Cai X J, Zhao G P and Kang L S 2016 *Chin. Phys. B* **25** 110301
[21] Liu F L and Zhao L B 2017 *Phys. Rev. A* **95** 043428
[22] Deng M, Gao W, Lu R, Delos J B, You L and Liu H P 2016 *Phys. Rev. A* **93** 063411
[23] Stodolna A S, Lépine F, Bergeman T, Robicheaux F, Gijsbertsen A, Jungmann J H, Bordas C and Vrakking M J J 2014 *Phys. Rev. Lett.* **113** 103002
[24] Chen X, Wu Y and Zhang J T 2017 *Phys. Rev. A* **95** 013402
[25] Wang L, Yang H F, Liu X J, Liu H P, Zhan M S and Delos J B 2010 *Phys. Rev. A* **82** 022514
[26] Mitchell K A, Handley J P, Tighe B, Flower A and Delos J B 2004 *Phys. Rev. A* **70** 043407
[27] Mitchell K A, Handley J P, Tighe B, Flower A and Delos J B 2004 *Phys. Rev. Lett.* **92** 073001
[28] Mitchell K A, Handley J P, Tighe B, Delos J B and Knudson S K 2003 *Chaos: An Interdisciplinary Journal of Nonlinear Science* **13** 880
[29] Mitchell K A, Handley J P, Delos J B and Knudson S K 2003 *Chaos: An Interdisciplinary Journal of Nonlinear Science* **13** 892
[30] Kotimäki V, Räsänen E, Hennig H and Heller E J 2013 *Phys. Rev. E* **88** 022913
[31] Yi X H, Bi J J, Liu R, Wang C K, Jiao Y and Li Z L 2016 *Chin. Phys. B* **25** 128503
[32] Byrd T A and Delos J B 2014 *Phys. Rev. E* **89** 022907
[33] Cai X J, Zhang Y H, Li Z L, Jiang G H, Yang Q N and Xu X Y 2013 *Chin. Phys. B* **22** 020501
[34] Mackay R S, Meiss J D and Percival I C 1984 *Physica D* **13** 55
[35] Zhang Y H, Cai X J, Li Z L, Jiang G H, Yang Q N and Xu X Y 2013 *Chin. Phys. Lett.* **30** 040501
[36] Mitchell K A and Steck D A 2007 *Phys. Rev. A* **76** 031403
[37] Friedman N, Kaplan A, Carasso D and Davidson N 2001 *Phys. Rev. Lett.* **86** 1518
[38] Mitchell K A and Delos J B 2006 *Physica D: Nonlinear Phenomena* **221** 170